Study of photon remnant in resolved interactions at HERA

Alice Valkárová [a]
for H1 Collaboration

[a]Nuclear Center of Charles University, V Holešovičkách 2, Praha 8,
180 00, Czech Republic

Events with a resolved photon, $x_\gamma < 0.75$, and two hard jets in the final state are used to study the transverse momentum of the photon remnant in photo – and low – Q^2 ($1.4 \leq Q^2 \leq 25$ GeV^2) production. The average transverse momentum of the photon remnant in the $\gamma^* p$ system is found to increase weakly with the virtuality Q^2 of the photon and with the scale of the hard subprocess. The results are satisfactorily simulated by the Monte Carlo program HERWIG.

1. Introduction

In lepton-lepton and lepton-hadron collisions [1], the incoming leptons can act as sources of virtual photons, which are subsequently probed in hard collisions with partons from the other beam particle. Hard scattering between an almost real photon and proton is expected, in lowest order of QCD, to occur by two different mechanisms. The photon may interact directly with a quark or gluon from the proton or it may fluctuate into quarks and gluons which then interact with the partons from the proton. These two processes are called direct and resolved, respectively.

In resolved processes only a fraction of the momentum of the photon is involved in the hard collision, while the remaining momentum is carried by spectator partons. These partons fragment into a photon remnant jet which is expected to be approximately collinear with the original photon. Therefore in most Monte Carlo simulations the resolved photon is modeled as a hadron with collinear incoming partons.

The photon remnant was studied by the ZEUS collaboration in photoproduction events [2] using k_t clustering algorithm. Its properties were found to be consistent with those commonly attributed to jets. The fraction of the incident photon's energy which is reconstructed in the photon remnant jet was analyzed by H1 in the region $0 \leq Q^2 \leq 49$ GeV^2 in [3]. The evolution of this fraction with Q^2 was found to be consistent with the picture of a resolved photon contribution which is suppressed with increasing virtuality.

In this paper, the properties of photon remnant jet are studied for photoproduction events and for events with low Q^2. The dependence of the p_t of the photon remnant jet on the virtuality Q^2 and the scale of an accompanying hard process are compared with Monte Carlo predictions.

1.1. Data selection

The analysis is based on data taken in 1995 with the H1 detector operating at the lepton-proton collider HERA, with positrons of 27.5 GeV colliding with protons of 820 GeV. The integrated luminosity used for this analysis is 1.05 pb^{-1}.

The events were selected according to the kinematic properties determined by measurements of the scattered positron and the hadronic final state. The following variables are used:

$$Q^2 = 4E_e E_e^{'} \sin^2(\theta^{'}/2),$$
$$y = 1 - E_e^{'}/E_e \cos^2(\theta^{'}/2), \qquad (1)$$

calculated from the positron beam energy E_e, the energy $E_e^{'}$ and the polar angle $\theta^{'}$ of the scattered positron.

In this analysis data samples with two different ranges of the virtuality Q^2 were used: photoproduction ($Q^2 < 10^{-2}$ GeV^2) and low Q^2 ($1.4 < Q^2 < 25$ GeV^2).

For both data samples, the z coordinate of the interaction vertex was required to be within 35 cm of the nominal position. The variable y was restricted to $0.25 < y < 0.7$ and $0.3 < y < 0.7$ for low Q^2 and photoproduction samples respectively.

To compensate for losses in the calorimetric measurement of hadrons, tracks reconstructed in the central drift chamber were used in addition to calorimetric clusters.

2. Photon remnant jet identification

It was shown [4] that the jet algorithm DECO is able not only to reconstruct jets from the hard process but also the photon remnant. In DECO jets are made by splitting the event into a sequence of subsets of particles, with the number of subsets running from 2 up to 5 ("jet multiplicity"). The decomposition into subsets (multiplets) is achieved by minimizing a jet function evaluated from the whole event. The jet function used here was thrust, extended up to 5 directions. DECO allows to reconstruct jets with any p_t and any mass.

In the process of jet finding with DECO we proceeded in the following way: since the photon remnant is defined as the remains of the incoming photon, we employ the trick of adding the auxiliary γ^* four–vector as an initiator vector for the photon remnant, which improves the resolution significantly. Initiators are also used in other jet algorithms, for example by the k_t algorithm. Then DECO decomposes every event into 4 jets in the laboratory system. It should be noted that DECO is fully Lorentz invariant [4]. The jet with the largest p_z component (relatively to the proton direction) is, as MC studies have shown, the proton spectator jet and is excluded from further analysis. Then we transform the jets from the laboratory to the $\gamma^* p$ system. The jet with the smallest p_z component in the $\gamma^* p$ system is assumed to be the candidate for photon remnant jet. Next we subtract the auxiliary virtual photon four–vector from the four–vector of the photon remnant jet candidate. When there was no other object in the photon remnant jet except for this auxiliary four–vector, then there is no photon remnant jet and the event is a direct photon candidate (note that in this limiting case $x_\gamma = 1$). If the photon remnant jet contains objects, the event is accepted as a candidate for the resolved photon process. The two other jets are then assumed to be jets from the hard process. These assumptions about the hard jets and the photon remnant jet are supported by MC studies shown later.

Events are now selected in which the two hard jets satisfy the conditions:

$$p_T^{(i)} \geq 5 \text{ GeV}, \quad -3 \leq \eta^{(i)} \leq 0, \qquad p_T^{(1)} + p_T^{(2)} > 12 \text{ GeV}, \tag{2}$$

where the transverse momenta $p_T^{(i)}$ and pseudorapidities $\eta^{(i)}$ are calculated in the $\gamma^* p$ system with the positive z–axis along the incident proton direction. An additional cut was applied to the difference in angles of the jets in the azimuthal plane, $|\varphi^{(1)} - \varphi^{(2)}| \geq 2$ rad.

The variable x_γ allows us to separate direct and resolved component with a reasonable accuracy. In our investigations we determined it using

$$x_\gamma = \frac{\sum\limits_{i=1}^{2} (E_i - p_{z,i})}{\sum\limits_{h=1}^{N} (E_h - p_{z,h})}, \tag{3}$$

where the sum runs over the two jets in the numerator and over all hadrons in the event in the denominator.

MC studies indicate that the $x_\gamma < 0.75$ region is dominated by the resolved component, with a small tail of direct component. Therefore, to enrich our data sample with resolved photon events the cut $x_\gamma < 0.75$ was applied.

3. Models

In this paper we used HERWIG [5] and RAPGAP [6] for the simulation of the direct as well as the resolved photon components.

For the photon parton density functions (PDF) of the virtual photon we use the GRV LO parameterizations for the real photon combined with the simple Drees–Godbole virtuality suppression factor [7]

$$L(Q^2, M^2, \omega^2) \equiv \frac{\ln((M^2 + \omega^2)/(Q^2 + \omega^2))}{\ln((M^2 + \omega^2)/\omega^2)}, \tag{4}$$

where M is the hard scale and ω a free parameter should be fitted to data. The PDF's of the virtual photon are obtained from those of the real photon by multiplying the latter by L in the case of quarks and by L^2 in the case of gluons.

The distribution of the intrinsic momentum p_t of the partons in the photon and the proton (at the beginning of the initial parton showers) was taken as Gaussian

$$\mathrm{d}N/\mathrm{d}p_t^2 \propto \exp(-p_t^2/k_0^2) \tag{5}$$

with $k_0 = 0.66$ GeV in both HERWIG and RAPGAP.

It is well known that properties of jets with moderate p_T are significantly influenced by additional soft particles accompanying the basic parton level hard scattering but not originating from it. In HERWIG these soft particles are optionally generated via the mechanism called *soft underlying event* (SUE). We recall that there is no such additional mechanism in RAPGAP.

4. Corrections to acceptance and resolution

Events generated with the HERWIG MC were passed through a detailed simulation of the H1 detector and were used to correct for detector resolution and acceptance. The parameter regulating the amount of the soft underlying event activity in HERWIG was determined from the study of the transverse energy flow outside the jets and from jet profiles to be $0.1-0.2$ [8]. We used 0.2 (0.15) for the photoproduction (low Q^2) sample, respectively. The value $\omega = 0.2$ GeV (used in eq. (4)) was found to give a reasonable description of dijet cross sections with HERWIG and RAPGAP [9]. The HERWIG has been used to study the effects of the detector smearing. In Figure 1 the correlation between the x_γ as reconstructed in the detector and the x_γ as determined from the hadonic final state is shown: good correlation is observed in this variable as well as in $p_T^{(1)} + p_T^{(2)}$. The correlation for p_t, azimuthal angle φ and the pseudorapidity η of the photon remnant jet is also satisfactory, as seen in Figure 2. Because of the good correlation between detector and hadron level distributions and the

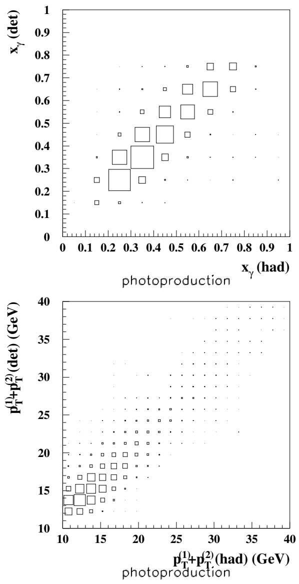

Figure 1. The correlation of x_γ and $p_T^{(1)} + p_T^{(2)}$ of the two hard jets at the hadron and detector level (photoproduction sample of HERWIG).

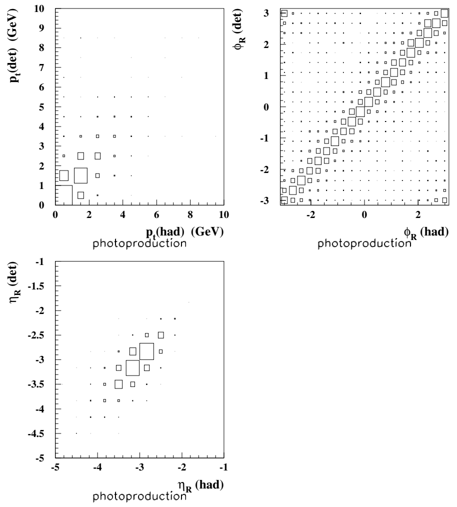

Figure 2. The correlation of p_t ,φ_R and η_R of the photon remnant jet at the hadron and detector level (photoproduction sample of HERWIG).

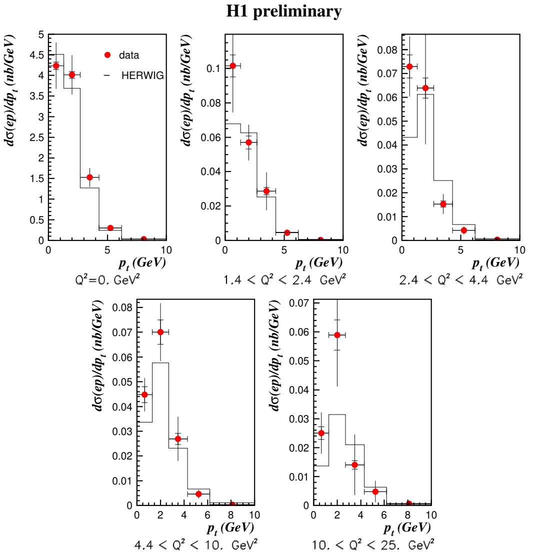

Figure 3. The differential cross section $d\sigma/dp_t$ of the photon remnant jet for the data (points) and HERWIG (histogram) in intervals of the photon virtuality Q^2.

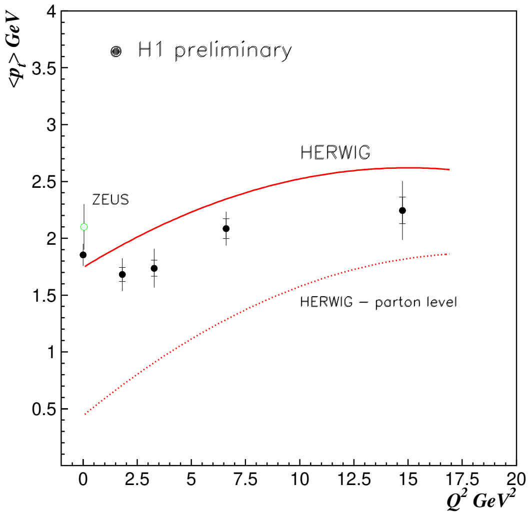

Figure 4. The mean p_t value of the photon remnant jet for data (points) and HERWIG (curves), as a function of the photon virtuality Q^2. (Cut for resolved events: $x_\gamma < 0.75$, hard jet cuts: $p_T^{(i)} > 5$ GeV, $-3 < \eta^{(i} < 0$ (i=1,2) and $p_T^{(1)} + p_T^{(2)} > 12$ GeV.)

satisfactory description of the data by MC (not shown here), HERWIG can be used to correct the measured photon remnant distributions for acceptance and resolution effects of the detector.

The p$_t$ distribution of the photon remnant jet was corrected using an unfolding procedure [10] based on Bayes theorem.

Resolved events were defined by requiring $x_\gamma <$ 0.75. However, as MC studies have shown, in this region of x_γ we still have a tail of direct events – at the level of a few percent, depending on Q^2. The uncertainty of the determination of this background was included in the systematic error and is less than 7% for both data samples.

The largest sources of systematic errors were the unfolding procedure uncertainty (< 10%), the uncertainty connected with the subtraction of direct processes (< 7%) and the scale uncertainty of the hadronic energy in calorimeters (< 5%).

5. Results

In Figure 3 the corrected differential cross sections dσ/dp_t of the photon remnant jet are presented for different intervals of photon virtuality Q^2 for data and HERWIG. In Figure 4 the corrected mean p$_t$ values for data and HERWIG are shown as a function of Q^2. A fit to $a + bQ^2$ gives a=1.79 ± 0.08 and b=0.03 ± 0.02, which is compatible with a weak increase with Q^2. HERWIG qualitatively describes the observed Q^2 dependence. The $< p_t >$ of the photon remnant jet of HERWIG at the parton level, as also displayed in Fig. 4, shows a similar rise with Q^2, albeit at a lower value. It suggests that the hadronization in HERWIG increases $< p_t >$ but does not change much the shape of the parton level dependence. We can compare our photoproduction value of $< p_t >= 1.85 \pm 0.10$ GeV with the ZEUS result of $< p_t >= 2.1 \pm 0.2$ GeV. Within errors the results are the same. The ZEUS experiment has used the k_T jet algorithm and a sample of events with hard jets with $p_T^{(i)} > 6$ GeV and $\eta_i < 1.6$, in the laboratory frame [2]. The corrected differential cross sections dσ/dp_t of the photon remnant jet are shown for four different intervals of the hard scale, $p_T^{(1)} + p_T^{(2)}$, in Figure 5 and Fig-

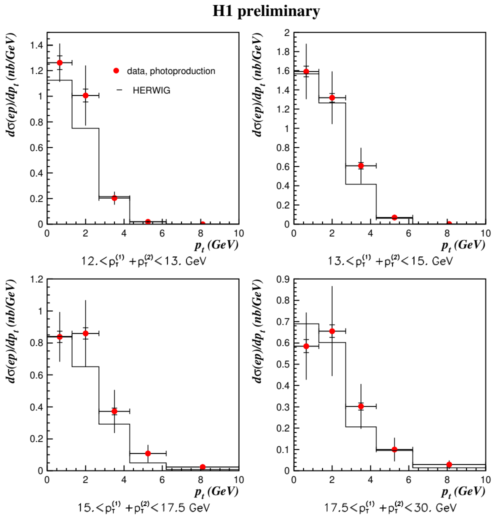

Figure 5. The differential cross section $d\sigma/dp_t$ of the photon remnant jet for the photoproduction data (points) and HERWIG (histogram) in intervals of the hard scale $p_T^{(1)} + p_T^{(2)}$.

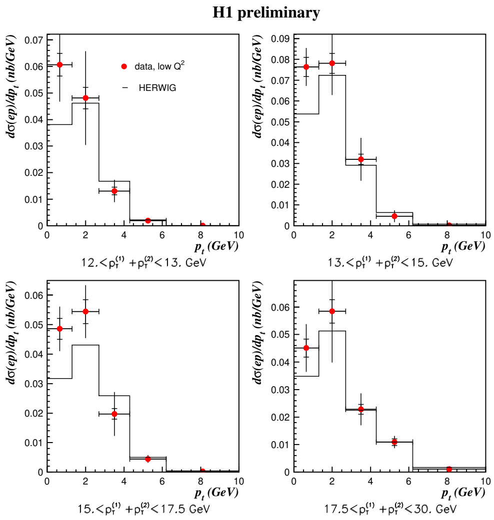

Figure 6. The differential cross section $d\sigma/dp_t$ of the photon remnant jet for low Q^2 data (points) and HERWIG (histogram) in intervals of the hard scale $p_T^{(1)} + p_T^{(2)}$.

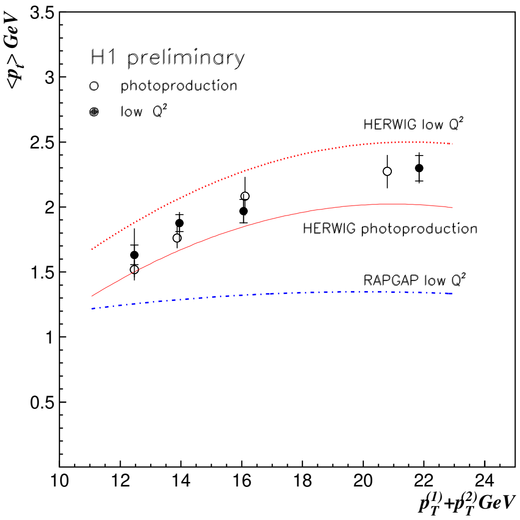

Figure 7. The mean p_t of the photon remnant jet for photoproduction (circles) and low Q^2 (full circles) data as a function of the hard scale $p_T^{(1)} + p_T^{(2)}$ compared with HERWIG and RAPGAP predictions. (Cut for resolved events: $x_\gamma < 0.75$, hard jet cuts: $p_T^{(i)} > 5$ GeV, $-3 < \eta^{(i)} < 0$ (i=1,2) and $p_T^{(1)} + p_T^{(2)} > 12$ GeV.)

ure 6 for photoproduction and the low Q^2 sample, respectively, together with the HERWIG predictions. In Figure 7 the corrected mean p_t values for both data samples are compared with results from HERWIG and RAPGAP. We can conclude that the $< p_t >$ is rising with increasing $p_T^{(1)} + p_T^{(2)}$ for data. Moreover, the dependence seems to be the same within errors for the photoproduction and low Q^2 samples. In order to check that the rise in mean p_t with the hard scale of the jets is not caused by energy from the hard jets leaking into the proton remnant jet, events were discarded for which the distance $R = \sqrt{\Delta\varphi^2 + \Delta\eta^2}$ between the remnant jet and each one of the two hard jets was less than 2. The remaining events displayed a similar clear rise as the full sample. HERWIG shows a similar dependence on the hard scale, however, it predicts smaller values of $< p_t >$ for photoproduction and larger ones for the low Q^2

sample. RAPGAP, using the same intrinsic p_t distribution (eq. (5)) with the same parameter $k_0 = 0.66$ GeV as used in HERWIG, gives too small mean values of p_t and no dependence on the scale $p_T^{(1)} + p_T^{(2)}$.
It was checked that the rise of $< p_t >$ with $p_T^{(1)} + p_T^{(2)}$ in HERWIG is not due to the presence of the soft underlying event activity . Furthermore the mean value of p_t was found to depend very weakly on the value of the parameter k_0 in HERWIG. The most important process which was found to be responsible for the magnitude of the mean $< p_t >$ and its dependence on the hard scale is the presence of initial parton showers.

6. Conclusions

The $\mathrm{d}\sigma/\mathrm{d}p_t$ distributions and the mean p_t of the photon remnant jet have been studied with the H1 detector for both photoproduction and low Q^2 data. They have been measured as a function of the photon virtuality Q^2 and the scale $p_T^{(1)} + p_T^{(2)}$ of the two hard jets in the event and they have been compared to the HERWIG MC model. In general HERWIG gives a more satisfactory description of the data than RAPGAP.

The mean p_t of the photon remnant jet is found to be compatible with a weak increase with Q^2 as might be expected from a photon shrinking with Q^2.

A clear increase of the mean p_t is found for increasing scale $p_T^{(1)} + p_T^{(2)}$ of the hard subprocess. This dependence is found to be the same, within errors, for both photoproduction and low Q^2 data.

REFERENCES

1. OPAL Collaboration, R. Ackers et al., Z. Phys. C61 (1994) 199;
   ALEPH Collaboration, D. Buskulic et al., Phys. Lett. B313 (1993) 509;
   DELPHI Collaboration, P. Abreu et al., Phys. Lett B342 (1995) 402;
   ZEUS Collaboration, M. Derrick et al., Phys. Lett. B322 (1994) 287;
   H1 Collaboration, T. Ahmed et al., Nucl. Phys. B445 (1995) 195;
   H1 Collaboration, S. Aid et al., Z. Phys. C70 (1996) 17;
   ZEUS Collaboration, M. Derrick et al., Phys. Lett. B348 (1995) 665;
   ZEUS Collaboration, M. Derrick et al., Phys. Lett B384 (1996) 401;
   ZEUS Collaboration, J. Breitweg et al., Eur. Phys. J. C1 (1998) 109;
   H1 Collaboration, C. Adloff et al., Eur. Phys. J. C1 (1998) 97.
2. ZEUS Collaboration, M.Derrick et al.,Phys. Lett. B 354 (1995) 163.
3. H1 Collaboration, C. Adloff et al., Phys. Lett. B415 (1997) 418.
4. A. Valkárová, G.Knies Comparison of Cone and Event-Decomposition Algorithms in Resolved Photon Reactions, DESY 94-047 (1994).
5. G. Marchesini et al., Comp. Phys. Commmun. 67 (1992), 1.
6. H. Jung, Comp. Phys. Commun. 86 (1995) 147.
7. M. Drees, R. Godbole, Phys. Rev. D50 (1994) 3124
8. M. Taševský, PhD Thesis, Prague 1999, unpublished.
9. H1 Collaboration, *Measurement of Dijet Cross-Sections at Low Q^2 and the Extraction of an Effective Parton Density of the Virtual Photon*, DESY-98-205, 1998
10. G. D'Agostini, Nucl. Instr. Meth. A362 (1995) 487.